https://doi.org/10.31925/farmacia.2026.2.8 **ORIGINAL ARTICLE**

DESIGN, MOLECULAR DOCKING AND ADME STUDIES OF NEW NAPROXEN DERIVATIVES AS ESTROGEN RECEPTOR ANTAGONISTS

KANAR M. ALAWAD [1]*, ASMAA ADNAN ABDULNABI [1], JESSICA SHLIMOON HANNA [2], TIBA M. HAMEED [1], KANY A. ABDULQADER [1], HUMAM L. QUSAY [3], NOOR ALI HUSSEIN SABZI [4], ANWAR A. TAMER [5], HAWAZIN AZIZ HAMIM [6]

[1]*Department of Pharmaceutical Chemistry, College of Pharmacy, AI-Nahrain University, Baghdad, Iraq*
[2]*National Diabetes Center, Mustansiriyah University, Baghdad, Iraq*
[3]*College of Pharmacy, Al-Farabi University, Baghdad, Iraq*
[4]*Ministry of Health and Environments, Department of Health in Baghdad, Rusafa, Baghdad, Iraq*
[5]*Department of Pharmaceutical Chemistry, College of Pharmacy/University of Baghdad, Baghdad, Iraq*
[6]*Department of Pharmaceutical Chemistry, College of Pharmacy, Mustansiriyah University, Baghdad, Iraq*

**corresponding author: kanar.muthana@nahrainuniv.edu.iq*

Manuscript received: December 2025

Abstract

The design of new anticancer agents aims to develop powerful treatments with fewer side effects. Using the Genetic Optimization for Ligand Docking (GOLD) software, new naproxen-based compounds were designed and primarily screened for anticancer efficacy by interacting with the estrogen receptor, Protein Data Bank (PDB) code: 3ERT. The new derivatives can be synthesized by reacting naproxen with semicarbazide to form the intermediate (N) and then reacting the N with an aldehyde (Schiff base reaction) to produce the final compounds (N1A-N9A). To anticipate the pharmacokinetics of the designed compounds, computational approaches, including absorption, distribution, metabolism, and excretion (ADME) studies, were performed using the Swiss ADME server. In addition, all of the designed compounds met the rule of five for M.W., H-bond acceptor, and topological polar surface area (TPSA), but did not meet the H-bond donor and partition coefficient. Compounds (N9A, N4A) interacting with amino acids in the active pocket of docking studies of ligands with the ER-α protein (breast cancer protein) showed increased Piecewise Linear Potential (PLP) fitness values near the reference tamoxifen, suggesting potential activity. Throughout the simulation period, the molecule S2 exhibited stable fluctuations, with root-mean-square deviation (RMSD) values below 3 Å when modeled in the enzyme pocket.

Rezumat

Utilizând programul *Genetic Optimization for Ligand Docking* (GOLD), au fost proiectați noi compuși derivați din naproxen și evaluați preliminar pentru potențialul lor anticancerigen prin interacțiunea cu receptorul estrogenic, corespunzător structurii din *Protein Data Bank* (PDB), cod: 3ERT. Noii derivați pot fi sintetizați prin reacția naproxenului cu semicarbazidă, formând un compus intermediar (N), urmată de reacția acestuia cu o aldehidă (reacție de tip bază Schiff), pentru obținerea compușilor finali (N1A–N9A). Pentru a anticipa proprietățile farmacocinetice ale compușilor proiectați, au fost realizate analize computaționale privind absorbția, distribuția, metabolismul și excreția (ADME), utilizând serverul SwissADME. De asemenea, toți compușii proiectați au respectat regula celor cinci în ceea ce privește masa moleculară, numărul de acceptori de legături de hidrogen și aria polară topologică, însă nu au îndeplinit criteriile referitoare la numărul de donori de legături de hidrogen și la coeficientul de partiție. Compușii N9A și N4A, care interacționează cu aminoacizii din situsul activ în studiile de andocare moleculară ale ligandului cu proteina ER-α (proteină asociată cancerului de sân), au prezentat valori crescute ale parametrului *Piecewise Linear Potential fitness*, apropiate de cele ale compusului de referință tamoxifen, sugerând un potențial efect biologic relevant. Pe parcursul simulării, molecula S2 a prezentat fluctuații stabile, valorile deplasării medii pătratice menținându-se sub 3 Å.

Keywords: Schiff base, pharmacokinetics, estrogen receptor, molecular docking

Introduction

To create effective policies for cancer prevention, screening, and diagnosis, it is necessary to have a thorough understanding of cancer epidemiology, which can shed light on potential causes and population trends (1). The study of chronic inflammation and the mediators it releases as tumors form and spread is becoming increasingly important in cancer research. Nonsteroidal anti-inflammatory medications (NSAIDs) are now being studied for their potential as an anti-tumor therapeutic agent on a worldwide scale (2). Our current understanding of the functional relationship between inflammation and cancer began with Rudolf Virchow's 1863

hypothesis, according to which cancer develops at the site of persistent inflammation (3).

The molecular mechanisms through which NSAIDs exert their chemopreventive effects remain a topic of debate. The most widely held theory is that they lower prostaglandin levels by inhibiting cyclooxygenase (COX-1 and 2) (4). Greater prostaglandin E2 (PGE2) levels in breast cancer patients have been linked to COX-2 overexpression (5).

Interestingly, PGE2, a well-known prostaglandin derived from COX-2, alters the local tumor microenvironment to promote the growth and metastasis of cancer cells. Therefore, substances that are more effective at reducing PGE2 in cancer cells are particularly desirable (6). Inflammation plays a key role in the development and spread of tumors and is intimately linked to cancer (7). Chronic inflammation contributes to the development of cancer by encouraging angiogenesis, metastasis, and proliferation while also lowering the immune system's and chemotherapeutic drugs' responses. That's why anti-inflammatory drugs are essential for cancer therapy and prevention, whether used alone or in combination with chemotherapeutic agents (5).

The use of NSAIDs increases apoptosis and reduces cell migration, thereby disrupting the tumor microenvironment. These drugs have been associated with a decreased risk of developing cancer in a number of different cancer types, including those of the breast, prostate, colon, ovaries, and head and neck (6).

Since NSAIDs have been shown to be effective against cancer, and since there is strong support for the research and development of new scaffolds that can be used to enhance the potency and reduce the toxicity of these drugs, we must modify one of these compounds, naproxen, through molecular docking or other drug design strategies (7).

The assumed synthesis pathway for the intermediate compound (Oxadiazole derivative) by reacting naproxen with semicarbazide and the final compounds (N1A-N9A) by reacting (Oxadiazole derivative) with different aldehydes, as shown Figure 1.

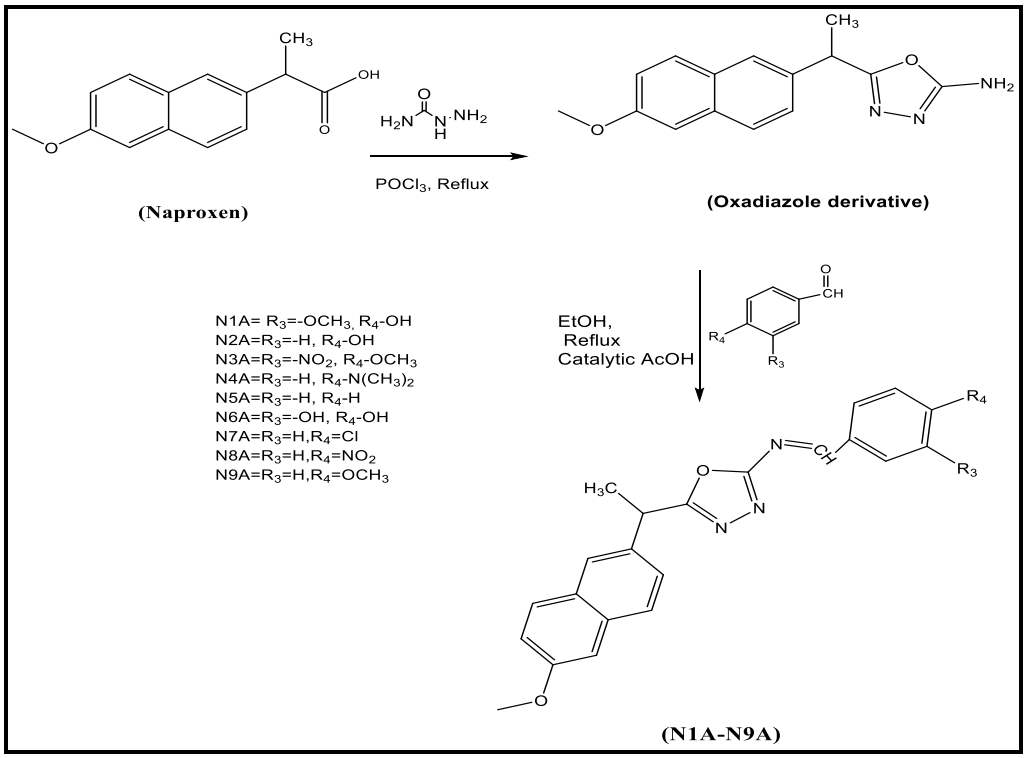

Figure 1.
Proposed synthesis scheme of naproxen derivatives

Materials and Methods

Computational strategies

For the suggested new chemicals, Swiss ADME has helped with ADME prediction. By using the docking method, it was possible to foretell the ligand's orientation and conformation about the target's binding site. All molecular docking studies were carried out on a high-performance workstation (MSI Summit E16Flip) equipped with a 13th Gen Intel® Core™ i7-1360P processor (2.20 GHz), 16 GB RAM, and an NVIDIA of the compounds' ADME, as well as other physicochemical parameters, were obtained from the Swiss GeForce RTX 4050 Laptop GPU, running Windows 11 Pro 64-bit.

ADME studies for final compounds

Studies ADME website (8). Using ChemAxon's Marvin JS software, the molecular blueprints of the novel compounds [N1A, N2A, N3A, N4A, N5A,

N6A, N7A, N8A, and N9A] were created. The Swiss ADME tool was used to convert these structures to SMILES, enabling the prediction of their physicochemical and pharmacokinetic properties. Lastly, this stage used the BOILED EGG to investigate the polarity, lipophilicity, passive gastrointestinal absorption, and brain uptake of the compounds (9).

Molecular docking studies for final compounds

Creating new compounds with desired pharmacological properties takes time and money, making drug discovery and development a significant challenge. Because many drugs become toxic or ineffective during later stages of clinical development, this cost has increased in part (10). Because computational technologies save researchers time, money, and effort, they are becoming more and more popular and are becoming indispensable in the pharmaceutical discovery and development process (11, 12). One of these methods for predicting the ligand's orientation and conformation inside the target's binding site is the docking approach (13). Accurate general structural modeling and a thorough comprehension of chemical activity are the primary objectives of docking studies (14). Docking studies were conducted for the proposed compounds using the GOLD (v5.7.1) program from the Cambridge Crystallographic Data Center (CCDC) (15). Photography, posture estimation, bond length estimation, interaction modes (hydrogen bonds or short contacts), and visualization of ligands, receptors, active sites, and active sites were all accomplished using the Hermes visualizer program (v.1.10.1) (16).

Setting up ligands and receptors

The chemical structures of the compounds were drawn using ChemDraw (v.16.0) (17). Next, we minimized the energy of our new molecules (18) using Chem3D (v.16.0) and the MM2 force field. Once that was done, the estrogen receptor-α (positive breast cancer) protein and the tamoxifen metabolite 4-hydroxytamoxifen (PDB code: 3ERT) were used as the active target's three-dimensional structure for docking ligands (19). The receptor was then imported from the PDB using the Hermes module of GOLD (20). The docking process might be confirmed by re-docking the co-crystallized ligands (21). The water molecules (HOH31, 58, and 68) that are necessary for the protein receptor to interact with the ligands were isolated after removing all water molecules outside the receptor's active site (ER-α) (22). The correct ionization and entry into tautomeric forms of the amino acid residues required the addition of hydrogen atoms (23).

The receptor was ready for docking using the Hermes visualizer tool from the CCDC GOLD suite. The protein binding site for the docking method was identified within the reference ligand's (10 Å) vicinity. The docking technique's variables were all initialized to their default settings (24). The highest-ranked answer was established as the default, early termination was not permitted, and ten created poses were retained. For scoring purposes, the piecewise linear potential (ChemPLP) is used (25). At the end, the findings were stored as PDB files. By analyzing the docked poses, optimal binding mode, and binding free energy, one might glean valuable insights. The optimal interaction between the proposed ligands and the receptor's amino acids (ER-α) has been determined by analyzing these data (26).

Molecular dynamics (MD) simulation

All MD simulations in this study were performed using the Desmond software package, applying standard protocols and default settings to ensure reliability and reproducibility (27). The starting structures consisted of the protein 3ERT and the complex with the custom-designed ligand (28). This complex was constructed by selecting the optimal binding pose of ligand pose 1, previously determined by molecular docking studies, and then importing the protein–ligand pairs into Desmond's Maestro interface for system setup and simulation (29). Upon import, the complex underwent a rigorous preparation process in Maestro (30). This included the addition of missing hydrogen atoms, assignment of correct protonation states according to physiological pH, and inspection for any incomplete residues or atoms (31).

All non-essential crystallographic water molecules and heteroatoms were removed to focus the simulation on the primary protein–ligand interactions, while any structurally important water molecules were retained as needed (32). The structures were then subjected to energy minimization using Desmond's internal algorithms, which efficiently relax local strains and resolve any unfavorable contacts within the system (33). Following energy minimization, the protein–ligand complex was placed in an orthorhombic simulation box, solvated explicitly with TIP3P water molecules to mimic the aqueous cellular environment (34). The box was constructed with at least 10 Å of padding around the entire solute to prevent artificial interactions due to periodic boundary conditions (35). To further replicate physiological conditions, sodium and chloride ions were introduced to achieve a final ionic strength of 0.15 M, and additional counter-ions were added as necessary to ensure overall charge neutrality (36). The OPLS4 force field was employed for all molecular representations, providing accurate and up-to-date parameterization for proteins and ligands alike (37). The system was then equilibrated and simulated under the default Desmond workflow, which involves an initial phase of NVT ensemble equilibration (constant number of particles, volume, and temperature) at 300 K, followed by a switch to the NPT ensemble (constant number of particles, pressure, and temperature) at 1 atmosphere and 300 K (38). This two-step

equilibration protocol allows the system to reach thermal and pressure equilibrium, thus ensuring a realistic starting point for production dynamics (39). The production MD simulations were conducted entirely under the NPT ensemble, which is the standard for modeling biological systems, as it maintains constant pressure and temperature conditions closely analogous to those inside living cells and tissues (40).

Each production run lasted 100 nanoseconds, with a time step of 2 femtoseconds, and trajectory data were recorded every 10 picoseconds for detailed subsequent analysis (41). Throughout the simulation, a comprehensive suite of analytical methods was employed to assess the stability and interaction dynamics of the complexes (42). The RMSD of both the protein backbone and the ligand was calculated to monitor conformational changes and overall stability (43).

The radius of gyration (Rg) was used to evaluate protein compactness, while the number and nature of hydrogen bonds between ligand-pose 1 and the protein binding sites were monitored as a key metric of binding strength and specificity (44). Additional interaction analyses were carried out to visualize and quantify the persistence of critical molecular contacts (45). All analyses were performed using built-in Desmond tools and Maestro visualization modules (46, 47).

Results and Discussion

Chemical Synthesis

To synthesize the newly designed compounds, naproxen must be cyclized to produce an N, and this N must react with an aldehyde (Schiff base reaction) to produce the desired compounds (N1A-N9A). The potential synthetic route anticipated for future studies is shown in Figure 1.

Interpretation of ADME results

The Swiss ADME server was utilized to predict the ADME and physicochemical properties of proposed compounds. Furthermore, ligands with an inadequate pharmacokinetic profile can be excluded using this useful, cost-free method (48). One of the many features of Swiss ADME is TPSA, which gauges how well drugs penetrate cells. Compounds with TPSA values less than 140 $Å^2$ indicate high permeability and bioavailability (49). TPSA values for all compounds were found to be less than 140 $Å^2$. With the exception of compound N3A, the majority of ligands were well absorbed in the digestive system, indicating that these compounds are highly absorbed. Furthermore, the average bioavailability score for all compounds is 0.55. The useful and significant parameter known as Lipinski's "rule of five" states, in short, that compounds that are to be taken orally should have certain properties like M.W. ≤ 500 Dalton, ≤ 5 H-bond donor, ≤ 10 H-bond acceptor, and octanol-water partition coefficient (log p) ≤ 5; otherwise, they would have low bioavailability and permeability and TPSA < 140 $Å^2$. As indicated in Table I, the results demonstrated that every designed compound complied with the rule of five in M.W., H-bond acceptor, and TPSA. Figure 2 displays the BOILED-EGG for designed compounds. Demonstrate that the other compounds are largely and passively absorbed from the gastrointestinal tract (GIT), while only the compound N4A crosses the blood-brain barrier (BBB). P-glycoprotein does not carry compound N4A in blue dots out of the central nervous system (CNS) cells, but it does carry compounds [N1A, N2A, N3A, N5A, N6A, N7A, N8A, and N9A] out of CNS cells. The presence of one compound N3A outside the plot suggests that it did not enter the BBB or get absorbed from the GIT.

These ADME predictions clinically support the notion that the selected compounds have a good chance of being effective oral therapies.

Table I

study results

Comp.	H-Donor	H-Accepter	MR	TPSA (Å)	GIT Absp.	BBB permeability	Bio Activity	Lipinski Violation
N1A	**7**	**7**	**119.57**	**89.97**	**High**	**No**	**0.55**	**Yes, 0 violation**
N2A	**1**	**6**	**113.08**	**80.74**	**High**	**No**	**0.55**	**Yes, 0 violation**
N3A	**0**	**8**	**126.34**	**11.56**	**Low**	**No**	**0.55**	**Yes, 0 violation**
N4A	**7**	**5**	**125.27**	**63.75**	**High**	**No**	**0.55**	**Yes, 0 violation**
N5A	**0**	**5**	**111.06**	**60.51**	**High**	**Yes**	**0.55**	**Yes, 0 violation**
N6A	**0**	**5**	**120.99**	**60.5**	**High**	**No**	**0.55**	**Yes, 1 Violation MLOGP >4.15**
N7A	**0**	**5**	**116.07**	**60.51**	**High**	**No**	**0.55**	**Yes, 1 violation MLOGP >4.15**
N8A	**0**	**7**	**119.88**	**106.33**	**High**	**No**	**0.55**	**Yes, 0 Violation**
N9A	**0**	**6**	**117.55**	**69.74**	**High**	**No**	**0.55**	**Yes, 0 Violation**

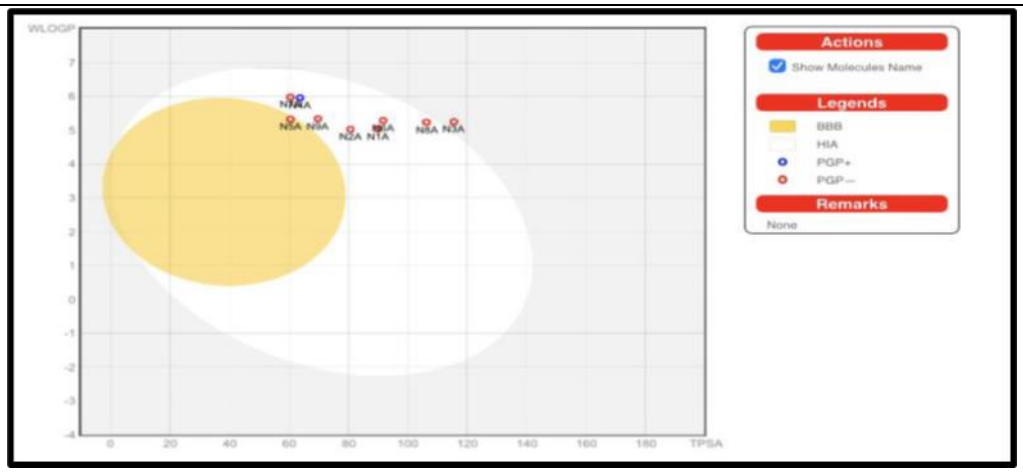

Figure 2.
BOILED-EGG for the designed compounds

Analysis of studies using molecular docking

GOLD stands for a "genetic approach through which flexible ligands are able to be docked within protein binding sites". GOLD generally yields excellent results in virtual screening and can predict posture. It can be purchased as part of the GOLD suite, which also includes a number of other software packages, such as Hermes, Mercury, ConQuest, GOLD, and Mogul (50).

To determine the most stable and energy-efficient conformation by altering the structure's geometry, methods for optimizing energy were developed. To determine the binding energies and specificity of the proposed compounds, docking studies examine the molecular interactions between the compounds and the active binding sites of proteins, including ER-α. The ER-α-inhibitory effects of tamoxifen and the proposed compounds have been evaluated using PLP fitness, which reflects complex formation at the active sites. The hydrogen-bond distance between our developed ligands and a specific protein was 3 Å, and the overall length of all bonds was 3 Å, according to the GOLD program (51, 52).

The results of the docking study for the reference and the highest PLP fitness compounds are displayed in Figures 3–6 and Table II, respectively. Excellent binding energies in the receptor's active region are displayed by [N1A, N2A, N3A, N4A, N5A, N6A, N7A, N8A, and N9A], which are also likely to positively interact with additional short contacts to reinforce the binding. In general, tamoxifen derivatives and naproxen derivatives function similarly. As can be seen in Table II and Figure 6, the naproxen derivative compound N9A with ER-α protein has the highest PLP fitness value of 86.794 overall according to the docking results. Compound N4A, the other naproxen derivative, yields an 86.6634 PLP fitness score when compared to the standard drug tamoxifen 97.8591, as illustrated in Figure 3. Based on docking results with the ER-α protein, compounds N9A and N4A yield the best scores of 87.694 and 86.6634, respectively. The re-docking of the reference ligand (4-hydroxytamoxifen) along with the protein (3ERT) was done, and the resulting RMSD was 1.161 A°, as this value is less than the accepted threshold of 2.0 Å, the docking process is validated and reliable.

Table II

The ER-α protein docked the binding energies of tamoxifen, a conventional medication, and naproxen derivatives

Compound	Binding energy (PLP) Fitness	Amino acid included in H- Bonding	Amino acid included in short contact
tamoxifen	97.85	GLY521(2), MET343 THR347(8), GLU419 LEU387(3), LEU408(1) ARG394(2), GLU354(5) LEU346	LEU525(2), GLY521(2) THR347(8), MET343 GLU419, LEU387 LEU408(2), ARG394(4) GLU353(6), LEU346
N1A	81.08	MET522(3), LEU525 MET343(2), THR347(7) GLU353(2)	MET522(3), TYR526(5) TRP383(4), LEU525 THR347(4), ALA350(2) GLU353(2)
N2A	76.71	LEU525(2), MET522(2) MET528, THR347(4) MET343, ALA350 PHE404	LEU525(3), MET522(4) TRP383, MET528 THR347(6), ALA350(2) PHE404, LEU346

Compound	Binding energy (PLP) Fitness	Amino acid included in H- Bonding	Amino acid included in short contact
N3A	84.10	PHE404(3), LEU346 PHE337, ALA350(2) THR347, ASP351 MET522(2), MET528	PHE404(4), ALA350(3) THR347(5), MET522(5)
N4A	86.66	THR347(6), LEU525(2) MET522(2), TYR526	ALA350(2), THR347(5) PHE404, LEU525(3) TYR526, MET522(3)
N5A	77.86	MET522(2), TYR526 LEU525(1), THR347 LEU346, MET342	MET522(2), TYR526 LEU525(2), ALA350(5) THR347(2), LEU346(2) PHE404, LEU391
N6A	79.16	LEU391(9), ARG394(5) LEU387(3), GLU353(5) THR347, TRP383(1) LEU536(2)	LEU391(9), ARG394(3) LEU387(3), GLU353(4) ALA350(5), LEU346(3) TRP383(1), LEU536(2)
N7A	81.50	MET522(2), LEU525(3) THR347(3), ASP351(1)	MET522(6), LEU525(3) THR347(3), ASP351(2)
N8A	82.73	MET522(4), LEU525(3) ASP351(3), THR347 LEU346	MET522(5), LEU525(5) THR347(2), ASP351(2) THR347, TRP383 LEU346
N9A	87.68	MET522(3), TYR526(2) LEU536(2), TRP383 LEU525, TRP383(2) THR347(9)	MET522(4), TYR526 LEU536(3), LEU525(2) TRP383, THR347(4)

*Numbers in brackets refer to the number of bonds.

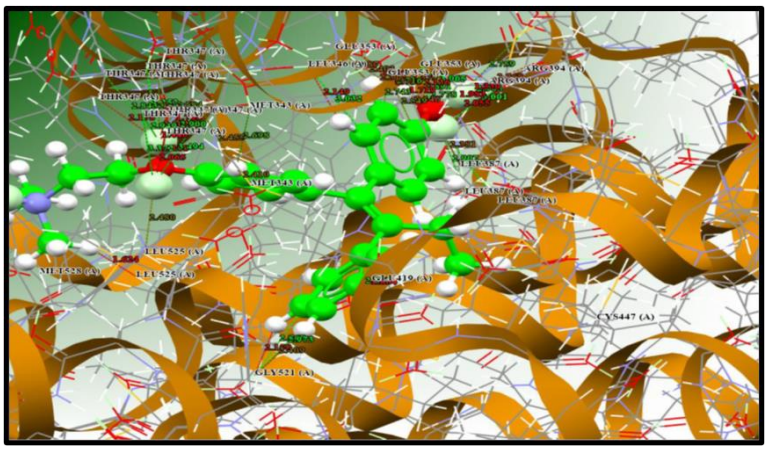

Figure 3.
Binding orientation and interaction of the tamoxifen compound inside the ER-α receptor

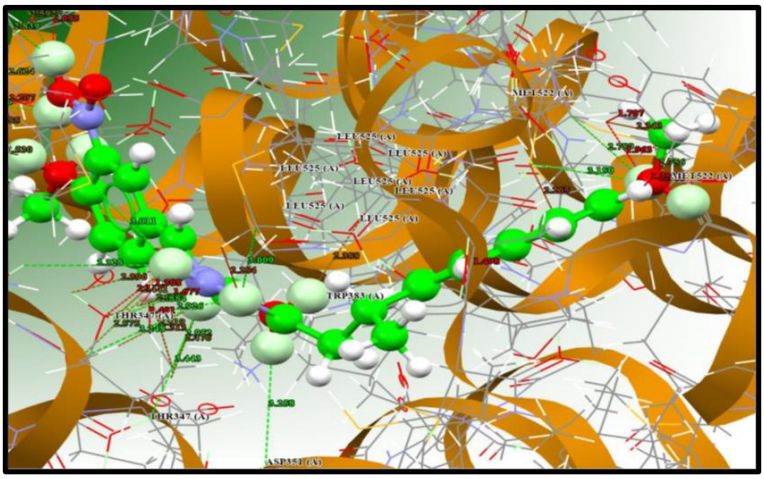

Figure 4.
Binding orientation and interaction of the N3A compound inside the ER- α receptor

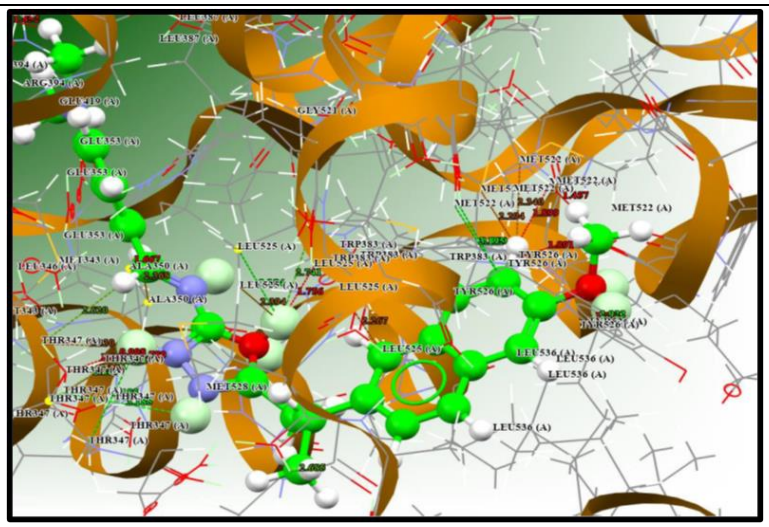

Figure 5.
Binding orientation and interaction of the N4A compound inside the ER- α receptor

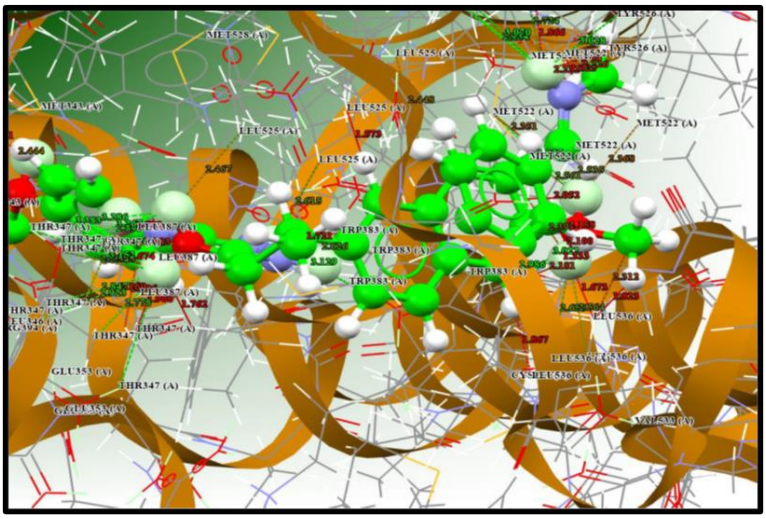

Figure 6.
Binding orientation and interaction of the N9A compound inside the ER-α receptor

MD Results

The technique of MD simulation represents a transformative leap in computational science, allowing researchers to observe and analyze the intricate atomic motions and interactions that dictate the behavior of biological macromolecules. The journey of MD began in the late 20th century, rooted in the need to transcend static representations of molecules and explore their true dynamism in a simulated environment (53). Early work by pioneers such as McCammon, Gelin, and Karplus in the 1970s laid the foundation for simulating the atomic fluctuations of proteins, marking a paradigm shift from static crystallographic snapshots to time-resolved molecular "movies". Over the past decades, advancements in computational power, algorithms, and force fields have enabled simulations of increasingly complex systems, spanning from small peptides to entire virus particles, and from nanoseconds to microsecond and even millisecond timescales (54). MD simulation is not merely a computational curiosity; it provides an unparalleled window into the "life" of a biomolecule. By solving Newton's equations of motion for thousands to millions of atoms, MD tracks how each atom moves under the influence of all the other atoms in the system and the environment (such as water and ions) (55). The MD trajectory indicates that the 3ERT–ligand complex reaches a stable equilibrium state after the initial equilibration phase. The RMSD (Figure 7) analysis shows a rapid deviation from the starting conformation, followed by a long plateau with a mean value of ~2.34 Å and limited fluctuations (SD ≈ 0.26 Å). This stable profile, without any sustained upward drift, confirms that the protein–ligand system maintains its global fold throughout the simulation. The final RMSD values being consistent with the late-window averages further validate the structural stability of the complex. The

RMSF (Figure 8) analysis supports these findings, demonstrating that the complex preserves a predominantly rigid scaffold with only localized flexibility. The average residue fluctuation (~1.16 Å) lies within the expected range for well-equilibrated nuclear receptor complexes (Figure 9). Peaks observed at residues such as CYS530, LYS529, and TYR526 correspond to loop or terminal regions that are naturally more dynamic. These flexible segments likely facilitate binding-pocket adaptability and solvent accessibility rather than indicating destabilization of the protein backbone.

Interaction analysis highlights the role of aromatic and electrostatic stabilization in the binding process. π–cation interactions occur in ~62% of frames, often involving up to two concurrent contacts, which provide electrostatic–π stabilization and help maintain the ligand orientation. π–π stacking interactions, while intermittent, appear repeatedly across the trajectory, reflecting natural side-chain breathing and conformational adjustments without disrupting the bound state. The persistence of these non-covalent interactions throughout the simulation reinforces the stability observed in the RMSD and RMSF profiles. Taken together, the RMSD, RMSF, and interaction analyses demonstrate that the 3ERT LBD remains structurally stable with the ligand bound, with only minor local motions that are essential for functional dynamics (Figure 10). The results support a binding mode characterized by a stable fold, localized flexibility, and recurring aromatic/π–cation interactions that collectively stabilize the ligand in the estrogen receptor binding pocket. Clinically, this binding stability supports the chance of sustained target binding, strengthening the potential of the compound as a reliable therapeutic candidate.

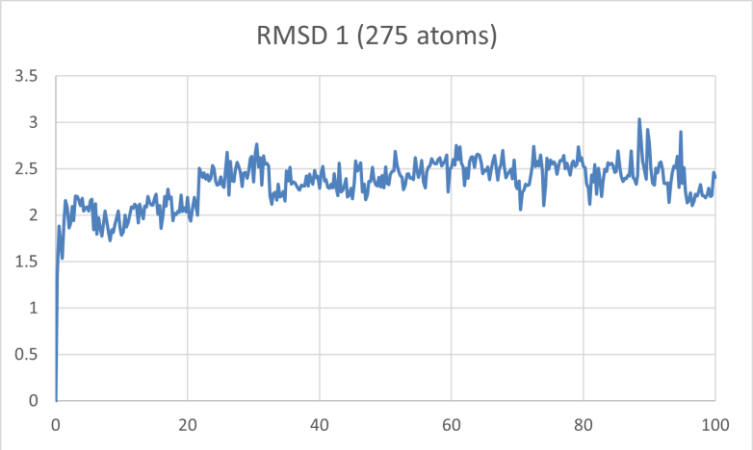

Figure 7.

A substantial spike in RMSD occurs in the initial nanoseconds when the system relaxes from its starting shape, followed by stability at 2.0-2.5 Å. After equilibration, the RMSD fluctuates slightly and spikes briefly before returning to baseline. This steady curve shows that the protein–ligand combination achieved equilibrium early and maintained a stable shape for 100 ns

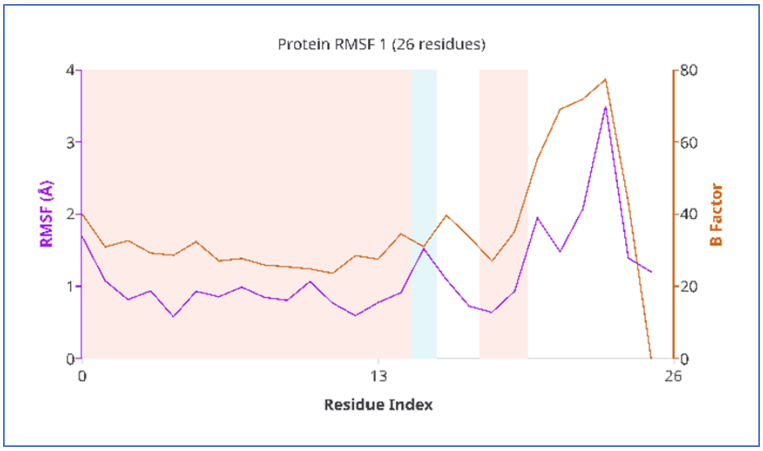

Figure 8.

RMSF and B-factor plot of the 3ERT–ligand complex showing most residues fluctuating within 0.6–1.2 Å, with peaks above 2.0 Å and up to 3.5 Å in the C-terminal region, indicating localized flexibility while overall stability is maintained

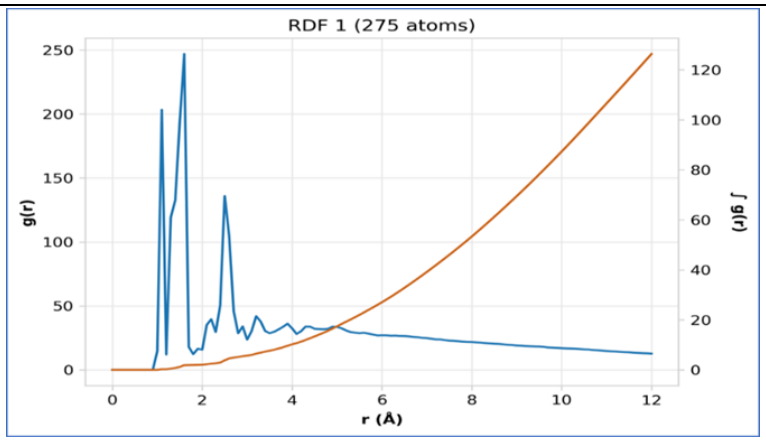

Figure 9.

Radial distribution function (RDF) plot of the 3ERT–ligand complex showing a major peak at 1.6 Å, minor coordination shells at 2.0–3.0 Å, and decay beyond 4–5 Å, indicating strong local interactions within the first coordination shell and bulk-like solvent behavior at larger distances

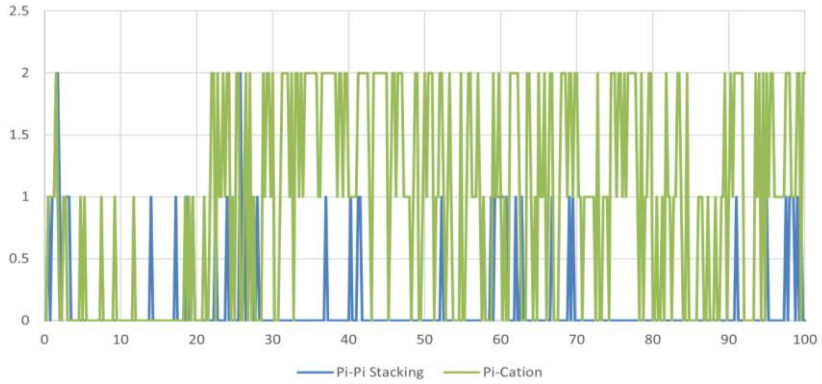

Figure 10.

Interaction plot of π–cation (green) and π–π stacking (blue) interactions during 100 ns simulation, highlighting their role in stabilizing ligand binding within the estrogen receptor pocket

Conclusions

It successfully developed a new series of naproxen compounds. [N4A, N9A] were the most promising compounds. About the same amount of activity as the anticancer drug tamoxifen is present in the compound (N9A). A combination of ADME investigations and *in silico* study predicted that all but one of the suggested compounds-N3A-would be highly absorbed from the GIT. According to ADME studies, every developed compound complied with the "rule of five" established by Lipinski. Promising outcomes were observed in docking studies investigating ligand interactions with the ER-α protein.

The MD results confirm that the 3ERT–ligand complex remains structurally stable, with RMSD (~2.34 Å, SD ≈ 0.26 Å) and RMSF (~1.16 Å) values indicating global rigidity and only localized flexibility in loop/terminal regions. Recurring π–cation (~62% occupancy) and intermittent π–π stacking interactions further stabilize the ligand orientation. Overall, the complex preserves its fold, maintains strong binding, and exhibits dynamic adaptability essential for receptor–ligand function.

Acknowledgement

The authors are grateful to Al-Nahrain University, College of pharmacy in Baghdad, Iraq; for their assistance in finishing this study.

Funding

This research received no external funding.

Availability of data and materials

The data generated and/or analyzed during the current study are included in this published article.

Ethics approval and consent to participate

Not applicable.

AI use disclosure

Not applicable.

Conflict of interest

The authors declare no conflict of interest.

References

1. Montagnana M, Lippi G. Cancer diagnostics: current concepts and future perspectives. Ann Transl Med. 2017;5(13):268.
2. Deb J, Majumder J, Bhattacharyya S, Jana SS. A novel naproxen derivative capable of displaying anti-cancer and anti-migratory properties against human breast cancer cells. BMC Cancer. 2014;14:567.
3. Ribatti D. Inflammation and cancer. In: Ribatti D, editor. Inflammation and Angiogenesis. Cham: Springer; 2017. p. 17-24.
4. Agrawal A, Fentiman IS. NSAIDs and breast cancer: a possible prevention and treatment strategy. Int J Clin Pract. 2008;62(3):444-449.
5. Zappavigna S, Cossu AM, Grimaldi A, Bocchetti M, Ferraro GA, Nicoletti GF, et al. Anti-inflammatory drugs as anticancer agents. Int J Mol Sci. 2020;21(7):2605.
6. Wong RSY. Role of nonsteroidal anti-inflammatory drugs (NSAIDs) in cancer prevention and cancer promotion. Adv Pharmacol Sci. 2019;2019:3418975.
7. Shi J, Leng W, Zhao L, Xu C, Wang J, Chen X, Wang Y, Peng X. Nonsteroidal anti-inflammatory drugs using and risk of head and neck cancer: a dose–response meta-analysis of prospective cohort studies. Oncotarget. 2017;8(58):99066-99074.
8. Cabrera N, Cuesta SA, Mora JR, Calle L, Márquez EA, Kaunas R, Paz JL. *In silico* searching for alternative lead compounds to treat type 2 diabetes through a QSAR and molecular dynamics study. Pharmaceutics. 2022;14(2):232.
9. Chedik L, Mias-Lucquin D, Bruyere A, Fardel O. *In silico* prediction for intestinal absorption and brain penetration of chemical pesticides in humans. Int J Environ Res Public Health. 2017;14(7):708.
10. DiMasi JA, Grabowski HG, Hansen RW. Innovation in the pharmaceutical industry: new estimates of R&D costs. J Health Econ. 2016;47:20-33.
11. Lionta E, Spyrou G, Vassilatis DK, Cournia Z. Structure-based virtual screening for drug discovery: principles, applications and recent advances. Curr Top Med Chem. 2014;14(16):1923-1938.
12. Macalino SJY, Gosu V, Hong S, Choi S. Role of computer-aided drug design in modern drug discovery. Arch Pharm Res. 2015;38(9):1686-1701.
13. Morris GM, Lim-Wilby M. Molecular docking. Methods Mol Biol. 2008;443:365-382.
14. Agu PC, Afiukwa CA, Orji OU, Ezeh EM, Ofoke IH, Ogbu CO, et al. Molecular docking as a tool for the discovery of molecular targets of nutraceuticals in diseases management. Sci Rep. 2023;13(1):13398..
15. Oyedele AK, Ogunlana AT, Boyenle ID, Adeyemi AO, Rita TO, Adelusi TI, et al. Docking covalent targets for drug discovery: stimulating the computer-aided drug design community of possible pitfalls and erroneous practices. Mol Divers. 2023;27(4):1879-1903..
16. Spackman PR, Turner MJ, McKinnon JJ, Wolff SK, Grimwood DJ, Jayatilaka D, et al. CrystalExplorer: a program for Hirshfeld surface analysis, visualization and quantitative analysis of molecular crystals. J Appl Crystallogr. 2021;54(3):1006-1011.
17. Yasotha S, Manivannan R, Sathya SR, Sankar K, Sathish Kumar P. Chemical structure and reaction schemes using chemdraw. Int J Pharm Anal Res. 2023;12(1):38-49.
18. Allinger NL. Conformational analysis. 130. MM2. A hydrocarbon force field utilizing V1 and V2 torsional terms. J Am Chem Soc. 1977;99(25):8127-8134.
19. Muchtaridi M, Syahidah HN, Subarnas A, Yusuf M, Bryant SD, Langer T. Molecular Docking and 3D-Pharmacophore Modeling to Study the Interactions of Chalcone Derivatives with Estrogen Receptor Alpha. Pharmaceuticals (Basel). 2017;10(4):81.
20. Berman HM, Westbrook J, Feng Z, Gilliland G, Bhat TN, Weissig H, et al. The Protein Data Bank. Nucleic Acids Res. 2000;28(1):235-242.
21. Wang R, Lai L, Wang S. Further development and validation of empirical scoring functions for structure-based binding affinity prediction. J Comput Aided Mol Des. 2002;16(1):11-26.
22. Nguyen A, Huang YC, Tremouilhac P, Jung N, Bräse S. ChemScanner: extraction and re-use(ability) of chemical information from common scientific documents containing ChemDraw files. J Cheminform. 2019;11(1):77.
23. Case DA, Cheatham TE 3rd, Darden T, Gohlke H, Luo R, Merz Jr KM, et al. The Amber biomolecular simulation programs. J Comput Chem. 2005;26(16):1668-1688.
24. Ravindranath PA, Forli S, Goodsell DS, Olson AJ, Sanner MF. AutoDockFR: Advances in Protein-Ligand Docking with Explicitly Specified Binding Site Flexibility. PLoS Comput Biol. 2015;11(12):e1004586.
25. Verdonk ML, Cole JC, Hartshorn MJ, Murray CW, Taylor RD. Improved protein–ligand docking using GOLD. Proteins. 2003;52(4):609-623.
26. Meng XY, Zhang HX, Mezei M, Cui M. Molecular docking: a powerful approach for structure-based drug discovery. Curr Comput Aided Drug Des. 2011;7(2):146-157.
27. Bowers KJ, Chow E, Xu H, Dror RO, Eastwood MP, Gregersen BA, et al. Scalable algorithms for molecular dynamics simulations on commodity clusters. Proceedings of the ACM/IEEE Conference on Supercomputing; 2006 Nov 11-17; Florida. New York: Association for Computing Machinery; 2006. p. 84-es.
28. Shiau AK, Barstad D, Loria PM, Cheng L, Kushner PJ, Agard DA, et al. The structural basis of estrogen receptor/coactivator recognition and the antagonism of this interaction by tamoxifen. Cell. 1998;95(7):927-937.
29. Iványczi M, Balogh B, Kis L, Mándity I. Molecular dynamics simulations of drug-conjugated cell-penetrating peptides. Pharmaceuticals (Basel). 2023;16(9):1251.
30. Sastry GM, Adzhigirey M, Day T, Annabhimoju R, Sherman W. Protein and ligand preparation: parameters, protocols, and influence on virtual screening enrichments. J Comput Aided Mol Des. 2013;27(3):221-234.
31. Olsson MHM, Søndergaard CR, Rostkowski M, Jensen JH. PROPKA3: consistent treatment of internal and surface residues in empirical pKa predictions. J Chem Theory Comput. 2011;7(2):525-537.

32. Levitt M, Park BH. Water: now you see it, now you don't. Structure. 1993;1(4):223-226.
33. Shivakumar D, Harder E, Damm W, Friesner RA, Sherman W. Improving the prediction of absolute solvation free energies using the next generation OPLS force field. J Chem Theory Comput. 2012;8(8):2553-2558.
34. Jorgensen WL, Chandrasekhar J, Madura JD, Impey RW, Klein ML. Comparison of simple potential functions for simulating liquid water. J Chem Phys. 1983;79(2):926-935.
35. Kasahara K, Sakuraba S, Fukuda I. Enhanced sampling of molecular dynamics simulations of a polyalanine octapeptide: effects of the periodic boundary conditions on peptide conformation. J Phys Chem B. 2018;122(9):2495-2503.
36. Li H, Robertson AD, Jensen JH. Very fast empirical prediction and rationalization of protein pKa values. Proteins. 2005;61(4):704-721.
37. Lu C, Wu C, Ghoreishi D, Chen W, Wang L, Damm W, et al. OPLS4: improving force field accuracy on challenging regimes of chemical space. J Chem Theory Comput. 2021;17(7):4291-4300.
38. Frenkel D, Smit B. Understanding molecular simulation: from algorithms to applications. 2nd ed. San Diego (CA): Academic Press; 2002.
39. Karplus M, McCammon JA. Molecular dynamics simulations of biomolecules. Nat Struct Biol. 2002;9(9):646-652.
40. Lindahl E, Sansom MSP. Membrane proteins: molecular dynamics simulations. Curr Opin Struct Biol. 2008;18(4):425-431.
41. Dror RO, Dirks RM, Grossman J, Xu H, Shaw DE. Biomolecular simulation: a computational microscope for molecular biology. Annu Rev Biophys. 2012;41:429-452.
42. Hollingsworth SA, Dror RO. Molecular dynamics simulation for all. Neuron. 2018;99(6):1129-1143.
43. David CC, Jacobs DJ. Principal component analysis: a method for determining the essential dynamics of proteins. Methods Mol Biol. 2014;1084:193-226.
44. Grant BJ, Rodrigues APC, ElSawy KM, McCammon JA, Caves LSD. Bio3D: an R package for the comparative analysis of protein structures. Bioinformatics. 2006;22(21):2695-2696.
45. Lobanov MY, Bogatyreva NS, Galzitskaya OV. Radius of gyration as an indicator of protein structure compactness. Mol Biol (Mosk). 2008;42(4):623-628.
46. Schrödinger Release 2023-4: Desmond Molecular Dynamics System; Maestro Visualization Modules. New York (NY): Schrödinger, LLC; 2023.
47. Humphrey W, Dalke A, Schulten K. VMD: visual molecular dynamics. J Mol Graph. 1996;14(1):33-38.
48. Lipinski CA, Lombardo F, Dominy BW, Feeney PJ. Experimental and computational approaches to estimate solubility and permeability in drug discovery and development settings. Adv Drug Deliv Rev. 2001;46(1-3):3-26.
49. Daina A, Michielin O, Zoete V. SwissADME: a free web tool to evaluate pharmacokinetics, drug-likeness and medicinal chemistry friendliness of small molecules. Sci Rep. 2017;7:42717.
50. Jones G, Willett P, Glen RC, Leach AR, Taylor R. Development and validation of a genetic algorithm for flexible docking. J Mol Biol. 1997;267(3):727-748.
51. Verdonk ML, Cole JC, Hartshorn MJ, Murray CW, Taylor RD. Improved protein–ligand docking using GOLD. Proteins. 2003;52(4):609-623.
52. Lyne PD. Structure-based virtual screening: an overview. Drug Discov Today. 2002;7(20):1047-1055.
53. Norberg A, Nilsson L. Advances in biomolecular simulations: methodology and recent applications. Q Rev Biophys. 2003;36(3):257-306.
54. McCammon JA, Gelin BR, Karplus M. Dynamics of folded proteins. Nature. 1977;267(5612):585-590.
55. Guo M, Wang H, Potter SS, Whitsett JA, Xu Y. SINCERA: a pipeline for single-cell RNA-seq profiling analysis. PLoS Comput Biol. 2015;11(11):e1004575.